

The STAR Vertex Position Detector

W.J. Llope^{*,a}, J. Zhou^a, T. Nussbaum^a, G.W. Hoffmann^b, K. Asselta^c,
J.D. Brandenburg^a, J. Butterworth^a, T. Camarda^c, W. Christie^c,
H.J. Crawford^d, X. Dong^e, J. Engelage^d, G. Eppley^a, F. Geurts^a,
J. Hammond^c, E. Judd^d, D.L. McDonald^a, C. Perkins^d, L. Ruan^c,
J. Scheblein^c, J.J. Schambach^b, R. Soja^c, K. Xin^a, C. Yang^f

^a*Rice University, Houston, Texas 77005*

^b*University of Texas, Austin, Texas, 78712*

^c*Brookhaven National Laboratory, Upton, New York 11973*

^d*University of California, Berkeley, California 94720*

^e*Lawrence Berkeley National Laboratory, Berkeley, California 94720*

^f*University of Science & Technology of China, Hefei 230026, China*

Abstract

The 2×3 channel pseudo Vertex Position Detector (pVPD) in the STAR experiment at RHIC has been upgraded to a 2×19 channel detector in the same acceptance, called the Vertex Position Detector (VPD). This detector is fully integrated into the STAR trigger system and provides the primary input to the minimum-bias trigger in Au+Au collisions. The information from the detector is used both in the STAR Level-0 trigger and offline to measure the location of the primary collision vertex along the beam pipe and the event “start time” needed by other fast-timing detectors in STAR. The offline timing resolution of single detector channels in full-energy Au+Au collisions is ~ 100 ps, resulting in a start time resolution of a few tens of picoseconds and a resolution on the primary vertex location of ~ 1 cm.

Keywords: Vertex position detector, time resolution

PACS: 25.75.Cj, 29.40.Cs

* Corresponding author. *E-mail address:* llope@rice.edu.

1. Introduction

In full-energy, $\sqrt{s_{NN}}=200$ GeV, Au+Au collisions at the Relativistic Heavy-Ion Collider (RHIC), pulses of tens to hundreds of photons from π^0 decays stream outwards from the primary collision vertex at the speed of light and very close to the beam pipe. A detector capable of measuring the arrival times of these photons can thus provide important information for event triggering, especially on the location of the primary vertex along the beam pipe, and on the time that the event occurred relative to free-running master clocks used by other fast timing detectors in the experiment. In the Solenoidal Tracker at RHIC (STAR) [1], the first detector capable of such measurements that was implemented was the “pseudo Vertex Position Detector” (pVPD) [2]. This system consisted of two identical assemblies of three readout detectors, one on each side of STAR (east and west), with each assembly mounted immediately outside the beam pipe. The pVPD worked well in full-energy Au+Au collisions [2]. However, for lighter beams such as p+p and also Au+Au beams at lower beam energies, the efficiency of the pVPD for providing the vertex location and the event time degraded due to the relatively lower multiplicities of very forward prompt particles in such collisions. To address this, the pVPD was upgraded to increase the readout detector channel count on each side of STAR in the same acceptance. This detector is called the Vertex Position Detector (VPD).

Unlike the pVPD, the VPD has been fully integrated into the STAR trigger system. The VPD provides the primary detector input to the STAR minimum bias trigger in A+A collisions. Each VPD assembly measures up to nineteen times in each event. These times are thus available, both online and offline, to measure the location of the primary vertex along the beam pipe, Z_{vtx} , via the equation,

$$Z_{vtx} = c(T_{east} - T_{west})/2, \quad (1)$$

where T_{east} and T_{west} are the times from each of the two VPD assemblies and c is the speed of light. The event “start time,” which is needed by the STAR Time-of-Flight (TOF) and Muon Telescope Detector (MTD) [3] systems to perform particle identification at mid-rapidity, is given by,

$$T_{start} = (T_{east} + T_{west})/2 - L/c, \quad (2)$$

where L is the distance from either assembly to the center of STAR.

One motivation for the increased channel count from the pVPD to the VPD in the same angular acceptance was to increase the efficiency of the detector for recording hits in single events. Another important motivation involves the fact that the experimental resolution on either T_{east} or T_{west} used in equations (1) and (2) improves like $1/\sqrt{N}$, where N is the number of channels on each side that were hit by prompt particles. That is, taking T_{east} or T_{west} as the average over all channels hit by prompt particles in an event results in a resolution on, *e.g.*, Z_{vtx} , given by,

$$\sigma(Z_{vtx}) = (c/2)\sigma_{\Delta T} = (c/\sqrt{2})\sigma_T = (c/\sqrt{2})\sigma_0/\sqrt{N}, \quad (3)$$

where T is T_{east} or T_{west} , $\sigma_{\Delta T}$ is the resolution of the time difference $T_{east}-T_{west}$, σ_T is the resolution on T_{east} or T_{west} , and σ_0 is the time resolution of a single readout detector. The larger channel count in the VPD thus allows an averaging over a larger number of lit channels and hence an improved performance for measuring both Z_{vtx} and T_{start} . The larger number of readout channels also provides more time values in the same acceptance, allowing one to better recognize which times are prompt and which times should be rejected as (delayed) outliers. The rates for such non-prompt hits are nearly negligible in full-energy Au+Au collisions, but are significant for p+p and lower energy Au+Au collisions.

This paper is organized as follows. Section 2 describes the design of the detectors and the electronics. Section 3 describes the configuration of the system for a new RHIC beam, the offline calibration of the detectors, and the start-timing and Z_{vtx} performance. Finally, Section 4 presents the summary and conclusions.

2. Design

The VPD exists as two identical detector assemblies, one on the east and one on the west of STAR. The design of these assemblies is described in section 2.1. Each of the nineteen detectors used in each assembly is composed of a Pb converter followed by a fast, plastic scintillator which is read out by a photomultiplier tube (PMT). The signals from the nineteen detectors in each assembly are digitized independently by two different sets of electronics which are described in section 2.2.

The detector was first installed in advance of the 2007 RHIC run. The bases for the PMTs were revised before the 2008 RHIC run. The detector has been used without additional modifications in every RHIC run since then.

2.1. Detectors

Each VPD assembly consists of nineteen detectors, a side view of which is shown in Figure 1. Each detector housing is a 2 inch outer diameter and 0.049 inch thick aluminum cylinder with 3/8 inch thick aluminum front and back caps. Inside this cylinder is a 0.25 inch non-conducting spacer, then the active elements consisting of a 0.25 inch (1.13 radiation lengths) Pb converter, and a 1 cm thick scintillator (Eljen EJ-204) coupled to a 1.5 inch diameter Hamamatsu R-5946 mesh dynode PMT via RTV-615 optically transparent silicone adhesive. The PMTs used in the VPD were taken from the TOFp detector [2] after it was decommissioned in 2005.

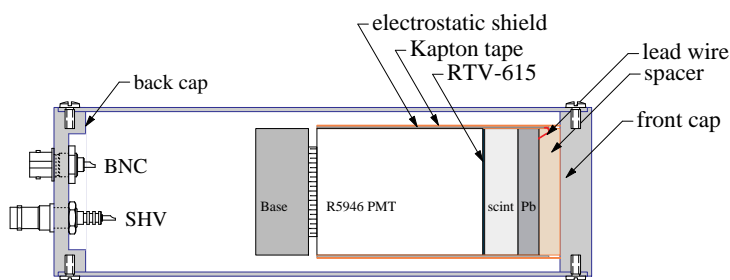


Figure 1: A schematic side view of VPD detector. The signal and high voltage connectors on the back cap are not shown.

The PMT dynode voltages are provided by a conventional linear resistive base. An initial version of these bases was used in the 2007 RHIC run, and the detectors performed well, but there was some “ringing” in the trailing edge of the PMT line shapes. This slightly complicated the offline slewing corrections, but did not affect the timing performance. In 2008, these bases were revised. No changes were made to the component values or connections, but the placement of these components was revised to minimize the lengths of the traces inside each PMT base circuit board. The excessive trace lengths in the previous version of the bases resulted in enough distributed inductance to cause the trailing edge ringing, which was completely removed in the final bases.

A wire connects the PMT cathode pin to a 0.001 inch thick aluminum cylinder which extends past the active elements. Another wire is used to connect the aluminum cylinder to the lead converter. In this way, the active elements are enclosed on all but one side by an electrostatic shield. This shield is electrically isolated from the active elements inside and the alu-

minum outer cylinder outside by several layers of Kapton tape. The output coaxial connector shield is isolated from the detector housing and the high voltage ground but is indirectly connected via a 1 k Ω resistor. This prevents the (inductive) shield of the coaxial signal cable from forming an undesirable resonant circuit with the (capacitive) electrostatic shield and detector housing while maintaining the high voltage ground return path.

Each VPD assembly consists of two rings of readout detectors and is mounted to the I-beam that supports the STAR beam pipe. A front view of one of the VPD assemblies is shown in Figure 2. The outer diameter of the beam pipe at this distance is five inches. An assembly exists as two semi-annular “clam-shells” that enclose the beam pipe. These are bolted together and are held in place by Delrin support blocks which attach to a horizontal mount plate which is clamped to the beam pipe support I-beam. The beam pipe and I-beam are at a different (dirty) electrical ground than the experiment, so the Delrin support blocks both hold the assembly in place and electrically isolate it.

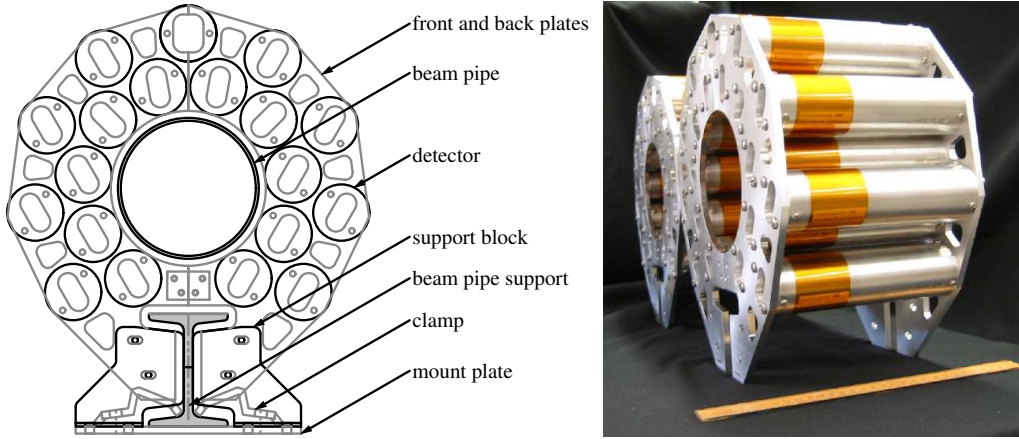


Figure 2: On the left is a schematic front view of a VPD assembly, and on the right is a photograph of the two VPD assemblies. A one foot long ruler is shown for scale on the right.

The two assemblies are mounted symmetrically with respect to the center of STAR at a distance of 5.7 m. The nineteen detectors in each assembly subtend approximately half of the solid angle in the pseudo-rapidity range of $4.24 \leq \eta \leq 5.1$. When viewed from the rear and looking towards the center of STAR, the detectors are numbered 1-10(11-19) counter-clockwise starting

from the lower right in Figure 2 in the inner(outer) ring.

2.2. Electronics

The signals from the VPD detectors are digitized by two different sets of electronics. A schematic view of the components that are involved is shown in Figure 3.

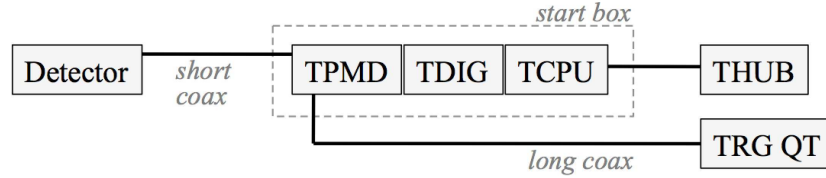


Figure 3: A schematic view of the VPD electronics and read-out paths.

The signals from the VPD detectors are connected via low-attenuation [2] Belden 9310 RG-58 “short coaxial” cables to “TPMD” boards which are mounted inside an aluminum “start box” that is positioned within ~ 6 feet of the VPD detector assemblies. Also mounted inside this box are the “TDIG” and “TCPU” boards. Digital data are sent over Category-6 cables to “THUB” boards, which then transmit the data over optical fiber to receivers in the STAR data acquisition system [4]. Additional details on these electronics boards can be found in Refs. [3] and [5].

The TPMD boards split the detector signals after they pass a diode-based clamping circuit which limits the pulse height to 4V. One output undergoes a leading-edge discrimination of these signals with respect to a tunable threshold at typically 25 mV. The Maxim MAX9601 comparator outputs are sent to the TDIG boards which use the CERN HPTDC chip [6] to digitize the arrival times of the signals with respect to an externally-input free-running clock. Each TDIG board uses three HPTDC chips in “very-high resolution” mode. The digitized times are 21 bit data words with a dynamic range of $52 \mu\text{s}$ and a least significant bit (LSB) time conversion of $25\text{ns}/1024 \approx 24.4 \text{ ps}$. The pulse sizes are measured by the TDIG boards as the width of the pulse at the threshold, which is called the “Time over Threshold” (ToT). All 2×19 channels of the VPD are digitized in these electronics.

The HPTDC chips exhibit a timing cross-talk [7] of up to three LSB when two signals arrive at the same HPTDC chip within a few nanoseconds of each other. To avoid this, there are five TPMD+TDIG board pairs in each start box, and each board pair handles only 3-4 detector channels out of the 24

possible. When two detector channels are connected to the same HPTDC chip, the “short coax” input cables are staggered in length in 12 ns steps so as to remove the possibility of HPTDC timing cross-talk.

The other signal from the passive split performed in the TPMD boards is passed on with negligible attenuation and distortion since the stub feeding the high impedance comparator is very short. This signal is sent over long (~ 100 ft) coaxial cables to electronics in the STAR trigger system called “QT boards” [8]. Short sections of coaxial cable are used after the TPMD boards and before these “long coax” cables to equalize the signal arrival times at the QT electronics to a few nanoseconds given the presence of the short coax cable staggering before the TPMD boards used to avoid the HPTDC cross-talk.

The QT boards are 9U VME boards and are part of the STAR Trigger system [9]. They perform pulse area and time measurements using an analog-to-digital (ADC) and time-to-amplitude-conversion (TAC) circuitry for all of the STAR trigger detectors. The ADC and TAC measurements are each 12-bit numbers. The TAC time measurement is common-stop with respect to the 9.4 MHz RHIC clock with a digital-to-time conversion of ~ 18 ps/LSB. For system design simplicity, only 2×16 channels of the VPD are digitized in QT boards.

3. Calibrations and performance

The information needed from the VPD for use in equations (1) and (2) are time values with the best possible experimental resolution. This first requires that the high voltage values used for each of the VPD PMTs result in equalized gains, *i.e.* the pulses from the different detectors should have the same size for the same amount of light generation in the scintillators. The time values digitized by the electronics described in section 2.2 include offsets resulting from propagation times inside the PMTs, signal cabling, and trace lengths in the electronics. There is also a dependence of the digitized pulse times on the size of the detector pulses which is called “slewing” [10]. The contributions from these sources of smearing are removed via offline calibrations of the VPD data. These calibrations, and the gain-matching of the VPD PMTs, is described in this section. The timing performance of the VPD detectors following these calibrations will also be presented in this section.

3.1. Configuration

RHIC is an extremely flexible machine. In the six runs (one per year) since the VPD was installed, it has provided p+p collisions at beam energies, \sqrt{s} , of 200 and 510 GeV, as well as Cu+Au, Au+Au, and U+U collisions at a number of beam energies, $\sqrt{s_{NN}}$, ranging from 7.7 to 200 GeV. The species and the number of particles per event producing signals in the VPD detectors depend strongly on the RHIC entrance channel and the collision centrality. In Au+Au collisions at 200 GeV, the signal in a VPD detector in one event is produced by $\gtrsim 10$ photons from π^0 decays and an approximately equal number of charged pions. In the lowest energy Au+Au collisions, *i.e.* 7.7 GeV, a VPD hit results from one or two spectator protons. The beam energy at which these trends cross depends on the centrality but is near 30-50 GeV according to URQMD [11] simulations. In similarity to the full-energy Au+Au collisions, VPD hits in p+p collisions result from a mixture of photons from π^0 's and charged pions, but unlike the full-energy Au+Au collisions, a VPD hit results from generally only one such particle per event. In order to provide consistently useful information from the VPD in these very different beam environments, the gains of the VPD PMTs must be set for each RHIC beam separately.

When a new beam is made available to the RHIC experiments, STAR sets up a simple interaction trigger generally based on the Zero Degree Calorimeter [9]. Using this trigger, data are collected from the VPD using three different sets of high voltage values, one at best guess values and the other two at ± 100 V with respect to the best guess values. The average ADC values from the TRG QT boards, $\langle ADC \rangle$, and the average ToT values from the TDIG electronics, $\langle ToT \rangle$, are measured for each of the three gain sets. The dependence of both quantities on the PMT high voltage value is fit with a power law for each channel. For the 2×16 VPD channels digitized by the trigger system QT boards, these functions are interpolated to determine the high voltage resulting in $\langle ADC \rangle = 300$. The relationship between the best high voltage values obtained from the $\langle ADC \rangle$ and $\langle ToT \rangle$ values is linear, which allows the gains for the 2×3 channels not digitized in the QT boards to be consistently set on the basis of the $\langle ToT \rangle$ values. The high voltage set-points so calculated are ~ 400 V lower in 200 GeV Au+Au collisions than they are in 200 GeV p+p collisions. The slopes of the power-law gain curves vary by 6-8% for the different detectors and are $\sim 5.8(7)$ in 200 GeV p+p(Au+Au) collisions.

Once the gains are set, data are collected to check the final gains and to

set the basic timing offsets in the QT boards. These offsets are determined by plotting the time in a VPD channel minus the average over the times in all other lit channels on the same side of STAR in the same event. The average values of these “1- $\langle N \rangle$ ” distributions are then set as the TAC offset values in the QT boards.

At this point, the VPD is commissioned for the new RHIC beam. Minimum bias triggers in STAR commonly use the VPD as the primary detector input. These triggers generally include constraints on the VPD time difference, *i.e.* equation (1), in order to enhance the rate for collisions near the center of STAR which have the best particle measurement efficiencies and the lowest backgrounds from particles produced in various detector support materials. These Z_{vtx} constraints are defined via upper and lower limits on the difference between the uncalibrated times from the earliest VPD hit on each side of STAR. Such an approach results in a Z_{vtx} resolution of ~ 5.5 cm in full-energy Au+Au collisions.

3.2. Slewing and offset calibrations

The integrated non-linearity in the HPTDC chips is corrected via code-density tests [5]. The smearing of the detector time values resulting from channel-dependent propagation delays, *a.k.a.* offsets, and from the slewing are removed via offline calibrations. The procedure is iterative, and results in a table of values binned by the pulse size, ToT, for each channel. In subsequent analyses, the event-by-event value of the pulse size in a lit detector in an event is used to look up a value from these tables which is subtracted from the raw value to remove the offsets and slewing. These calibration tables are determined as follows.

The events used are from the minimum bias trigger, often based on the VPD data itself, which requires that at least one VPD channel on each side of STAR is lit in an event. The location of the collision vertex along the beam pipe as reconstructed from the primary tracks in the STAR Time Projection Chamber (TPC) [12], Z_{vtx}^{TPC} , was required to be within ± 50 cm of the center of STAR. The transverse radius of the primary collision vertex was required to be less than 2 cm (inside the 2.5 cm radius beam pipe). At least two primary tracks were also required.

The first step involves the determination of initial relative offsets. These are obtained as the average values of the times in specific lit channels with respect to a reference channel (channel 1 on the west). Once these offsets are obtained, they are applied to the raw time values. The resulting time values

from a VPD channel minus the average of the times of all other lit channels on the same side of STAR in the same event are plotted as a function of that channel's ToT value. The dependence of the average “1- $\langle N \rangle$ ” times on each channel's ToT value is used in subsequent passes through the data to reduce the slewing and offsets. The procedure is iterative and determines three such calibration curves for each channel. The two VPD assemblies, one east and one west, are treated in parallel. The range of the dependence of the 1- $\langle N \rangle$ time differences on the ToT values is generally a few ns before the first pass, a few hundred ps before the second pass, and is negligible after the third pass. At the end of the procedure, the initial offsets and the three slewing correction tables for each channel are added together to produce the final correction tables versus the ToT values.

In full-energy Au+Au collisions, every VPD channel is hit by 10's of prompt particles in every event. As the beam energy of Au+Au collisions is decreased, the number of channels lit by prompt particles strongly decreases, and the probability that VPD channels are lit by non-prompt particles increases. These “late hit” channels must be rejected. This outlier rejection is performed as follows. The location of the primary vertex along the beam pipe calculated from the VPD times, Z_{vtx}^{VPD} , is calculated using equation (1) from every possible pair of lit channels with one channel on the east and one channel on the west. If the Z_{vtx}^{VPD} value from a pair of channels is consistent with the value of Z_{vtx}^{TPC} , these two channels are flagged as having prompt hits. This consistency is with respect to an analysis cut that becomes tighter in each calibration pass. It is also required that each of the N times used in the 1- $\langle N \rangle$ relative time calculation are consistent with the average values, $\langle N \rangle$, with a $\sim 4\sigma$ cut that also becomes tighter in each calibration pass.

Following the calibration procedure, the time resolution of a VPD channel after this procedure is called the single detector resolution, σ_0 , and is extracted as follows. Two dimensional plots of the “1- $\langle N \rangle$ ” time differences versus N are filled, and each bin of the N x-axis is fit with a Gaussian. The dependence of the standard deviations and mean values from these Gaussian fits as a function of N for a typical VPD channel is shown in the left frame of Figure 4. The solid line in this frame is the fit to the standard deviations using the functional form $\sigma(1-\langle N \rangle) = \sigma_0 / \sqrt{N/(N+1)}$, where the single detector resolution, σ_0 , is the fit parameter.

Important requirements of a successful VPD calibration are that the mean values of the “1- $\langle N \rangle$ ” time differences (open points) are near zero for all values of N , and that the standard deviations (solid points) follow the expected

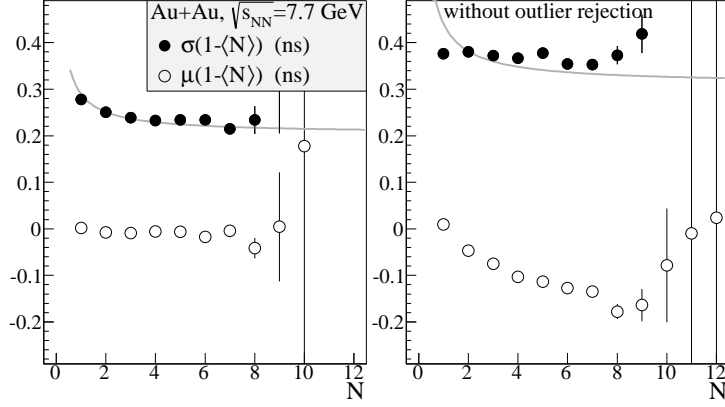


Figure 4: The average values (open circles) and standard deviation (solid circles) of the Gaussian fits to the “1- $\langle N \rangle$ ” time differences versus N for a typical VPD detector channel in the 7.7 GeV Au+Au data. The functional fit (see text) allowing the extraction of the single detector resolution, σ_0 , is shown as the solid line. In the left frame, the full outlier rejection is performed, and in the right frame, no outlier rejection is performed.

$\sigma_0/\sqrt{N/(N+1)}$ trend shown as the solid line in Figure 4. These requirements indicate the extent to which the VPD times measured by the different detector channels are self-consistent and result only from prompt particles. The right frame of Figure 4 shows the same standard deviations and mean values from the Gaussian fits to the 1- $\langle N \rangle$ time differences as a function of N but when no outlier rejection is performed. In this frame, the standard deviations (solid points) are ~ 100 ps larger and no longer follow the expected $\sigma_0/\sqrt{N/(N+1)}$ trend, and the mean values (open points) deviate significantly from zero. This underscores the importance of careful VPD time outlier rejection especially in p+p and low energy Au+Au collisions.

3.3. Performance

The single detector resolution, σ_0 , values extracted as described in the previous subsection are plotted versus the VPD channel number in Figure 5 for minimum bias data from a number of different RHIC entrance channels. The average values of the single detector resolution is 94 ps for full-energy Au+Au collisions, and increases to ~ 150 ps for intermediate energy Au+Au collisions and 510 GeV p+p collisions. The resolution for 7.7 GeV Au+Au collisions is approximately 200 ps, and is not shown as the VPD is generally not used to provide the start time to the TOF system due to its relatively low efficiency per event for those beams. The increasing single detector

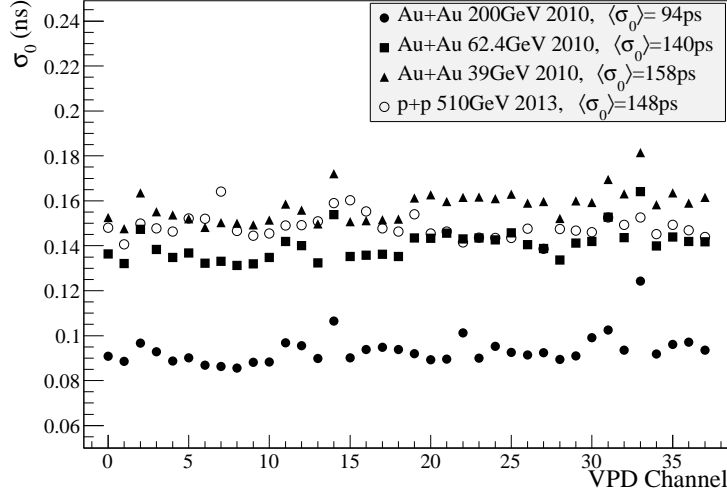


Figure 5: The single detector resolution versus the VPD channel number for a few recent RHIC beams and energies. The results for the VPD detectors on the west(east) are shown in the x-axis range 0-18(19-37).

resolution from full-energy Au+Au to the lower energy Au+Au and p+p collisions reflects the fact that the VPD is doing multiple-particle timing (per detector channel) in the highest energy Au+Au collisions and there is a gradual evolution to single-particle timing in p+p and lower energy Au+Au collisions.

The resolution by which the VPD measures the start time needed by the TOF and MTD detectors, *i.e.* equation (2), goes like $\sim \sigma_0 / \sqrt{M}$ where M is the total number of VPD channels lit by prompt particles in an event. In full-energy Au+Au collisions, the start time resolution is observed to be 20-30 ps, which is essentially negligible compared to the stop time resolution of the TOF(MTD) detectors of $\sim 80(100)$ ps [3]. In p+p collisions, the VPD start time resolution is approximately 80 ps, as for those beams σ_0 is ~ 150 ps and $M \approx 3$.

The resolution by which the VPD measures the primary vertex location is determined by comparing the VPD's measurement, Z_{vtx}^{VPD} (*i.e.* equation (1)), to that obtained from the primary tracks reconstructed in the TPC, Z_{vtx}^{TPC} . These two quantities are plotted in Figure 6 for 510 GeV p+p collisions (left frame) and 200 GeV Au+Au collisions (right frame). The insets in each frame depict the difference $\Delta Z = Z_{vtx}^{VPD} - Z_{vtx}^{TPC}$ and Gaussian fits to determine the vertex resolution. The standard deviations of these distributions obtained

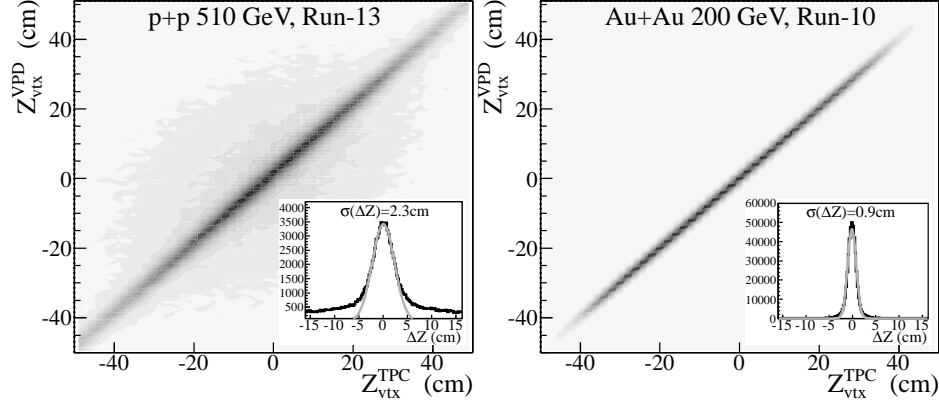


Figure 6: The primary vertex position along the beam pipe measured by the VPD, Z_{vtx}^{VPD} , versus the same position as obtained using the primary tracks reconstructed in the TPC, Z_{vtx}^{TPC} in 510 GeV p+p collisions (left frame) and 200 GeV Au+Au collisions (right frame). The insets depict the difference $\Delta Z = Z_{vtx}^{VPD} - Z_{vtx}^{TPC}$ which allows the extraction of the VPD's Z_{vtx} resolution as the standard deviation of the difference distributions.

from the fits are typically ~ 2.4 cm and ~ 1 cm in 510 GeV p+p collisions and 200 GeV Au+Au collisions, respectively.

4. Summary and conclusions

The 2×3 channel “pVPD” [2] vertex and start-timing detector in the STAR experiment at RHIC has been replaced by a 2×19 channel detector in the same acceptance. This Vertex Position Detector (VPD) exists as two identical assemblies, one on each side of STAR, very close to the beam pipe and ~ 5.7 m from the center of STAR. The readout channels in each assembly include a Pb converter followed by a fast plastic scintillator and a mesh dynode PMT. The PMT signals are digitized by two different sets of electronics for use in the STAR Level-0 trigger to select minimum bias collisions, to constrain the location of the primary collision vertex along the beam pipe, and to provide the start time needed by other fast timing detectors in STAR.

The system must be configured for each RHIC beam separately to provide a consistent performance despite the wide range of beam particles (protons to Au) and beam energies (7.7 to 510 GeV) provided by the RHIC. The slewing and offset corrections are performed using an iterative procedure and require a careful rejection of outlier times from non-prompt particles.

The single-detector resolution of the VPD, σ_0 , is approximately 95 ps in

full-energy Au+Au collisions, and degrades to ~ 150 ps in p+p and lower energy Au+Au collisions. The start time resolution of the VPD ranges from 20-30 ps in full-energy Au+Au collisions to ~ 80 ps in p+p collisions. The resolution by which the VPD can measure the location of the primary vertex in full-energy p+p and Au+Au collisions is ~ 2.5 cm and ~ 1 cm, respectively.

5. Acknowledgments

We thank the STAR Collaboration for the use of the experimental data shown in this paper and the operation of this system during RHIC running periods as part of STAR standard shift crew operations. We thank Allan Schroeder and the members of the UT-Austin machine shop for the machining of the structural parts of the detector assemblies. We appreciate the expert assistance of the BNL Collider-Accelerator department technicians Charlie Bloxson, Matt Ceglia, and Robbie Karl. We gratefully acknowledge funding from the US Department of Energy under Grant numbers DE-FG02-10ER41666 and DE-FG02-94ER40845.

References

- [1] K. H. Ackermann *et al.*, Nucl. Instr. Meth. A **499**, 624 (2003).
- [2] W.J. Llope *et al.*, Nucl. Instr. Meth. A **522**, 252 (2004).
- [3] W.J. Llope *et al.*, Nucl. Instr. Meth. A **661**, S110 (2012).
- [4] A. Ljubičić Jr. *et al.*, IEEE Trans. Nucl. Sci. **47**, 99 (2000);
J.M. Landgraf *et al.*, Nucl. Instr. Meth. A **499**, 762 (2003).
- [5] J.J. Schambach *et al.*, Int. J. Mod. Phys. E **16**, 2496 (2007).
- [6] M. Mota *et al.*, IEEE Journal of Solid-State Circuits **34**, 1360 (1999).
- [7] A.V. Akindinov *et al.*, Nucl. Instr. Meth. A **533**, 178 (2004).
- [8] H.J. Crawford *et al.*, <http://hena.lbl.gov/FMS/cap-equip-qt.pdf>
- [9] F.S. Bieser *et al.*, Nucl. Instr. Meth. A **499**, 766 (2003).
- [10] B. Bengtson and M. Moszyński, Nucl. Instr. Meth. **81**, 109 (1970);
B. Bengtson and M. Moszyński, Nucl. Instr. Meth. **158**, 1 (1979);
T. Sugitate *et al.*, Nucl. Instr. Meth. A **249**, 354 (1986).

- [11] S.A. Bass *et al.*, Prog. Part. Nucl. Phys. **41**, 225 (1998).
- [12] M. Anderson, *et al.*, Nucl. Instr. Meth. A **499**, 659 (2003).